

# **Technical evaluation of SenoBright HD contrast enhanced mammography functions of Senographe GE Pristina system**

Technical Report 2004

December 2020

Mary Kelly, Nicola Tyler, Alistair Mackenzie

## Acknowledgements

The authors are grateful to the staff at Guy's Hospital, London, for their assistance with the evaluation of this equipment.

## Funding

This study was funded for the NHS Breast Screening Programme by Public Health England.

# Contents

1. Introduction	4
1.1 Evaluation report	4
1.2 Objectives	4
1.3 Contrast enhanced mammography description	4
2. Methods	5
2.1 System tested	5
2.2 Phantoms	5
2.3 X-ray tube output and half value layer	7
2.4 Detector performance	7
2.5 Uniformity and artefacts	7
2.6 Automatic exposure control repeatability	7
2.7 Variation in AEC performance and image quality with phantom thickness	8
2.8 Mean glandular dose	8
2.9 Comparison of MGD between low energy CEM and standard 2D images	8
2.10 Subtraction of BR3D tissue equivalent material	8
3. Results	10
3.1 X-ray tube output and half value layer	10
3.2 Detector Performance	10
3.3 Uniformity and artefacts	11
3.4 Automatic exposure control repeatability	11
3.5 Variation in AEC performance and image quality with phantom thickness	12
3.6. Mean glandular dose	14
3.7. Accuracy of Indicated MGD	16
3.8. Comparison of MGD between Low Energy CEM and Standard 2D Images	16
3.9 Subtraction of BR3D Tissue-Equivalent Material	17
4. Discussion	18
4.1 Detector response and uniformity	18
4.2 Automatic exposure control	18
4.3 Mean glandular dose	18
4.4 Image quality	18
4.5 Image subtraction	18
5. Conclusions	19

# 1. Introduction

## 1.1 Evaluation report

At the time of publication of this report, the use of contrast enhanced mammography (CEM) is not approved for use in the NHS Breast Screening Programme (NHSBSP). Currently, the technology is being evaluated clinically. Further updates on approvals can be found on the PHE website:

<https://www.gov.uk/government/publications/breast-screening-status-of-approved-equipment>.

This report is one of a series evaluating the use of CEM on commercially available mammography systems and comprises a summary of the performance of CEM. There is currently no NHSBSP guidance on quality control testing of CEM systems. The methodology developed for this evaluation was primarily derived from two publications by Oduko et al.<sup>1,2</sup>

## 1.2 Objectives

The purpose of the evaluation was to assess the performance of the CEM SenoBright HD option for the GE Healthcare Senographe Pristina mammography system. The GE Pristina full field digital mammography system has previously been evaluated.<sup>3</sup>

## 1.3 Contrast enhanced mammography description

CEM involves the administration of an iodinated contrast agent followed by the acquisition of two images in close succession; the first at a low energy and the second at a higher energy. These exposures are designed such that the majority of X-ray energies in the spectra are either below or above the K-edge of iodine. An algorithm is then applied to create an image without breast structure that shows the location of any iodine accumulation. Such accumulation is a potential indicator of cancer.

## 2. Methods

The following describes the method for testing the CEM functions. Any system specific testing methods will be described in the results.

### 2.1 System tested

The system tested is described in Table 1.

**Table 1. System description**

Location	Guy's Hospital, London
Manufacturer	GE Healthcare
Model	Senographe Pristina
System Serial Number	000011171210217138
Anode target material	Rhodium (Rh), Molybdenum (Mo)
Additional filtration	30 $\mu\text{m}$ Ag, 30 $\mu\text{m}$ Mo, 0.25 mm Copper (Cu)
Detector type	Caesium Iodide
Detector size	Active imaging area not less than 233 mm x 285 mm
Pixel pitch	100 $\mu\text{m}$
Detector serial number	PXA0039_04
Software version	M3-3

### 2.2 Phantoms

#### CEM phantom

A phantom designed by Leithner et al<sup>4</sup> was used in the evaluation. The phantom consists of a 300 x 240 x 20 mm<sup>3</sup> PMMA block. Embedded within the phantom are 5 mm diameter discs containing Iopamidol at concentrations ranging from 0.25 to 2 mg cm<sup>-2</sup> of iodine. Discs containing 0 mg cm<sup>2</sup> iodine are also included in the phantom, as well as air-filled discs. Figure 1 shows an example subtracted image of the central region of the phantom whilst Figure 2 shows the composition of each disc within the matrix of 8 columns and 5 rows.

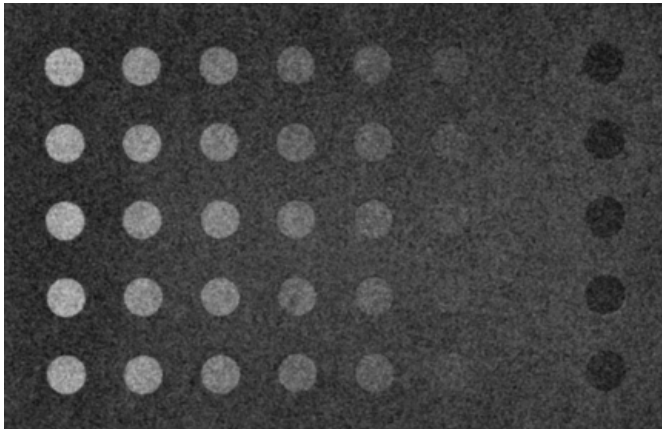


**Figure 1. Central region of subtracted image of CEM phantom**

2	1.5	1	0.75	0.5	0.25	0	Air
2	1.5	1	0.75	0.5	0.25	0	Air
2	1.5	1	0.75	0.5	0.25	0	Air
2	1.5	1	0.75	0.5	0.25	0	Air
2	1.5	1	0.75	0.5	0.25	0	Air

**Figure 2. Iodine concentration of each disc in CEM phantom in terms of mg cm<sup>-2</sup>. Discs in final column comprised of air.**

### Tissue equivalent blocks

The majority of the tests were undertaken using tissue equivalent blocks produced by CIRS (Norfolk, VA, USA). These blocks are designed to have similar attenuation properties as for specific fibroglandular densities of breast tissue. Dance *et al*<sup>5</sup> described a model to be used in breast dosimetry for a range of thicknesses from 20 to 110 mm. The model includes two 5 mm thick layers of fat at the upper and lower surface of the breast as well as an expected glandularity for the central portion of the breast. CIRS blocks of different densities by mass were selected to match as closely as possible those densities, in addition to the use of 5 mm of CIRS fat blocks at the bottom and top of the stack. Tables 2 and 3 show the combinations of blocks used to simulate the different breast thicknesses with and without the CEM phantom. Overall, a good match in density was found between the required glandularities and the actual values.

**Table 2. CIRS tissue equivalent material used for different phantom thicknesses in addition to two 5 mm thick fat blocks**

Total phantom thickness (mm)	Target glandularity of central area (%)	Glandularity of central portion (%)	CIRS Phantom [percentage glandularity] (mm)				
			Fat [0%]	30:70 [30%]	50:50 [50%]	70:30 [70%]	Glandular [100%]
20	100	100					10
30	72	70				20	
40	50	50			30		
50	33	33	10	20		10	
60	21	21	30	10		10	
70	12	12	50			10	
80	7	7	60		10		
90	4	4	70	10			

**Table 3. CIRS tissue equivalent material used for different phantom thicknesses in addition to CEM phantom**

Total phantom thickness (mm)	Target glandularity of central area (%)	Glandularity of central portion (%)	CIRS Phantom [percentage glandularity] (mm)				
			Fat [0%]	30:70 [30%]	50:50 [50%]	70:30 [70%]	Glandular [100%]
30	72	76%			10		
40	50	52%	10		10		
50	33	34%	20	10			
60	21	22%	40				
70	12	18%	50				

### 2.3 X-ray tube output and half value layer

The X-ray tube output and half-value-layer (HVL) were measured as described in the IPEM protocol<sup>6</sup> at intervals of 3 kV or, if only a limited number of options are used clinically, then only those options were measured.

### 2.4 Detector performance

Testing was carried out using 50 mm thick tissue equivalent material (Table 2) at the X-ray tube port and with the anti-scatter grid in position. The mean pixel value (PV) and standard deviation were measured in a region of interest. The relationships between mean PV and mAs, as well as variance and mAs, were then determined.

### 2.5 Uniformity and artefacts

Percentage non-uniformity was measured using unprocessed low and high energy images of the 25 mm thick PMMA block provided by GE for the flat field calibration of this system and following the methodology described in NHSBSP guidance.<sup>7</sup> Artefact evaluation was performed on low and high energy images as well as subtracted images. Images were viewed using a narrow window to examine any artefacts that may adversely affect clinical image quality.

### 2.6 Automatic exposure control repeatability

The CEM phantom was imaged with 30 mm thick breast equivalent tissue blocks (Table 3) to achieve a total thickness of 50 mm. The phantom was imaged under automatic exposure control (AEC). This was repeated until three sets of images were acquired.

Subtracted images were analysed to calculate the Signal Difference (SD), i.e. the difference in pixel value between each iodine disc and the background region. The contrast-to-noise ratio (CNR) for each disc was calculated by dividing the SD by the root mean square of the standard

deviation in the iodine disc and background region. The SDs and CNRs quoted in this report are the mean values for the five identical discs of each iodine concentration.

## 2.7 Variation in AEC performance and image quality with phantom thickness

The CEM phantom was imaged under AEC with varying combinations of tissue equivalent blocks, as shown in Table 3. Images were analysed to determine the SD and CNR for each iodine concentration.

## 2.8 Mean glandular dose

Exposures were carried out under AEC using the combinations of tissue equivalent blocks specified in Table 2. The exposure factors were noted and mean glandular doses (MGDs) were calculated for equivalent breast thicknesses using standard methods by Dance et al.<sup>5,8</sup>

The MGD indicated by the system was taken from the DICOM header for both exposures and compared with the calculated value.

## 2.9 Comparison of MGD between low energy CEM and standard 2D images

Images were acquired of the tissue equivalent blocks listed in Table 2 in standard 2D mode using AEC. MGDs were compared with those calculated for low energy CEM exposures.

## 2.10 Subtraction of BR3D tissue equivalent material

Small samples of iodine contained in a phantom were imaged with tissue-equivalent, heterogeneous material (CIRS BR3D phantom slabs, Figure 3) to assess whether the system could successfully subtract the tissue-like structures to reveal the iodine samples.



**Figure 3. CIRS BR3D phantom**

### 3. Results

#### 3.1 X-ray tube output and half value layer

The X-ray tube output and HVL measurements for the system in high energy mode are shown in Table 4. Measurements were performed with the compression paddle in the X-ray beam.

**Table 4. X-ray tube standard output and HVL measurements for high energy CEM image exposure parameters**

kV, Target/Filter	Tube Output ( $\mu\text{Gy/mAs @ 100 cm}$ )	HVL (mm aluminium)
49 kV Mo/Cu	2.59	3.15
49 kV Rh/Cu	2.89	3.06

#### 3.2 Detector Performance

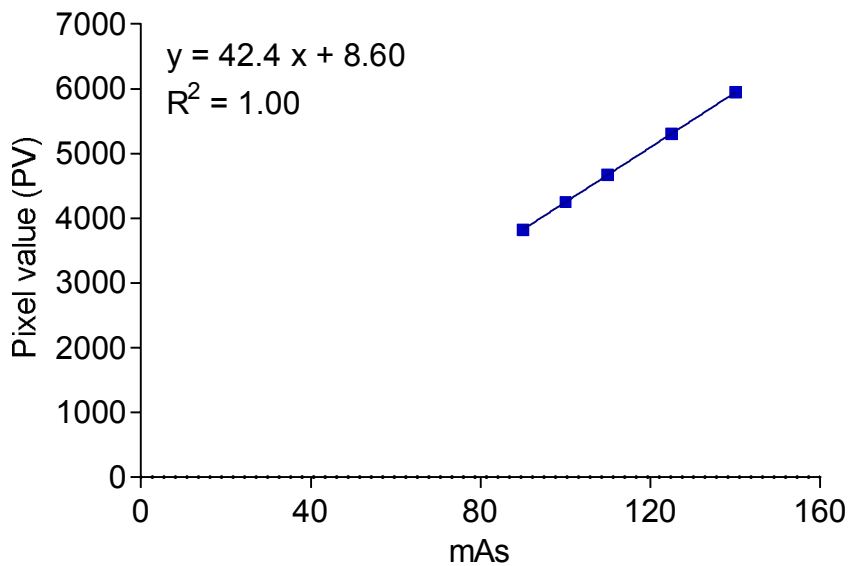


**Figure 4. Variation in pixel value of high energy CEM image with mAs**

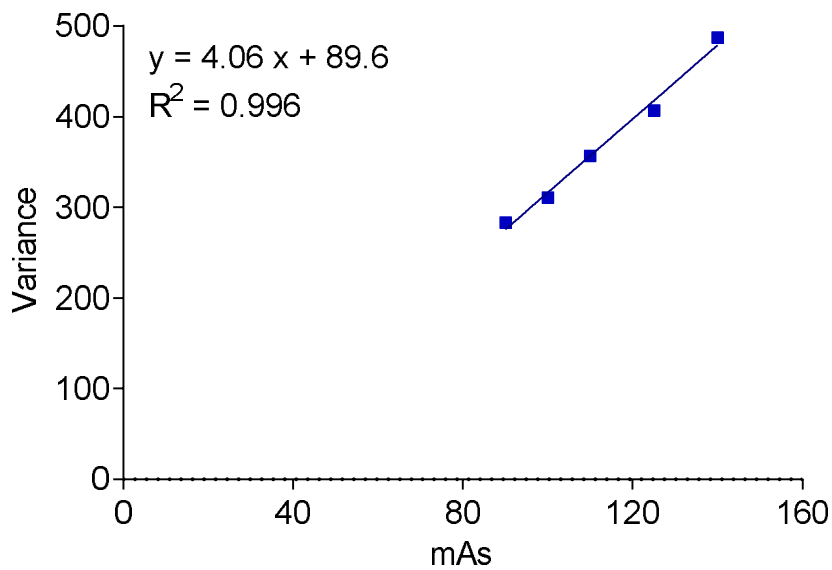


**Figure 5. Variation in high energy CEM image variance with mAs**

The exposures were acquired using 49 kV and a Rh/Cu target/filter combination. Figures 4 and 5 demonstrate that pixel value and variance (standard deviation squared) are linear with mAs (and hence detector dose) over this range of mAs values.

### 3.3 Uniformity and artefacts

The uniformity measurement was undertaken using the 25 mm thick PMMA block provided by GE for the flat field calibration of this system. Percentage non-uniformity was measured using unprocessed low and high energy images. The maximum variation in pixel value from the centre of the image was 1.6% and 1.2% for the low and high energy images respectively. Both values are below the NHSBSP remedial level of 10%.

Artefact evaluation was performed on low and high energy images as well as subtracted images. A faint ghosting artefact was seen on the unprocessed images, which is expected for this type of detector. A line structure was observed parallel to the chest wall on the high energy images; however, the signal variation in the structure was very small.

### 3.4 Automatic exposure control repeatability

Results for mAs, SD and CNR repeatability using “AOP STD” AEC mode are shown in Table 5. The mAs repeatability was within the NHSBSP recommended remedial tolerance of 5%.

**Table 5. Repeatability of mAs, SD and CNR for CEM exposures for 1.0 mg cm<sup>-2</sup>**

Max % variation from mean mAs	Low energy CEM exposure	0.2%
	High energy CEM exposure	0.1%
Max % variation from mean SD		1.8%
Max % variation from mean CNR		0.8%

### 3.5 Variation in AEC performance and image quality with phantom thickness

The SD and CNR results for 1.0 mg cm<sup>-2</sup> iodine for images acquired using “AOP STD” AEC mode are shown in Table 6, with results for other concentrations shown in Figures 6 and 7. For all iodine concentrations, the SD remains relatively constant with increasing phantom thickness when imaged in AEC mode (Figure 6). The CNR initially increases and then decreases with increasing phantom thickness, although CNRs are within ± 15% of the mean across the range of phantom thicknesses for 1.0 mg cm<sup>-2</sup> iodine. The SD and CNR increase linearly with iodine concentration for any given phantom thickness (Figures 7 and 8).

**Table 6. Variation in exposure parameters, SD and CNR for CEM subtracted images acquired in “AOP STD” AEC mode for 1.0 mg cm<sup>-2</sup>**

Phantom thickness (mm)	kV Target/Filter		SD	CNR
	Low energy exposure	High energy exposure		
20	26 kV Mo/Mo	49 kV Mo/Cu	40.7	2.9
30	26 kV Mo/Mo	49 kV Mo/Cu	40.5	3.1
40	34 kV Rh/Ag	49 kV Rh/Cu	42.2	3.4
50	34 kV Rh/Ag	49 kV Rh/Cu	41.1	3.0
60	34 kV Rh/Ag	49 kV Rh/Cu	42.7	2.9
70	34 kV Rh/Ag	49 kV Rh/Cu	42.3	2.7

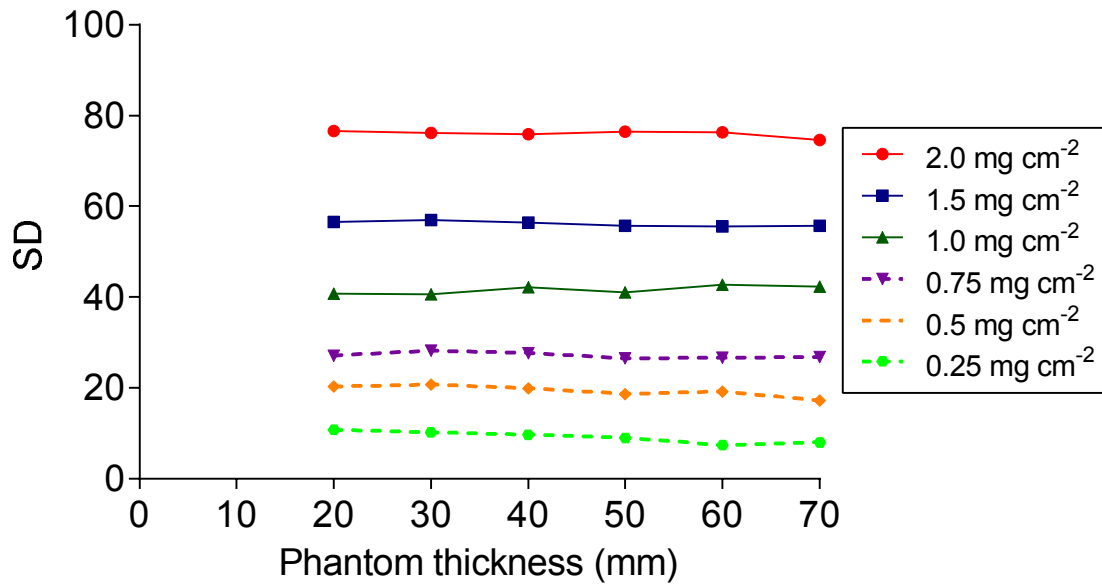


Figure 6. SD with varying phantom thickness for different concentrations of iodine (mg cm<sup>-2</sup>)

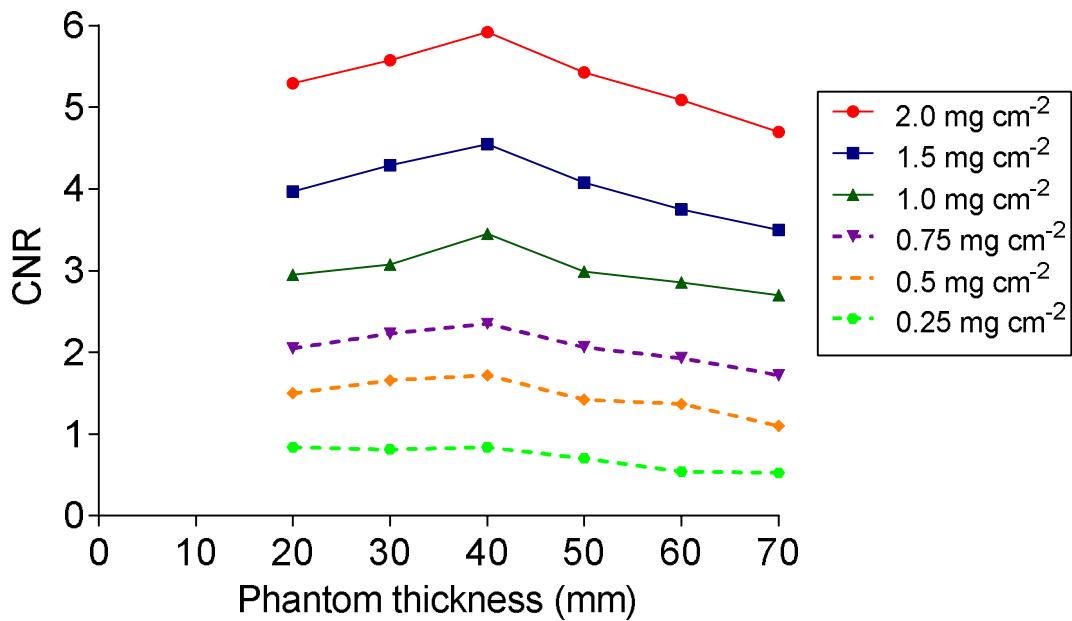
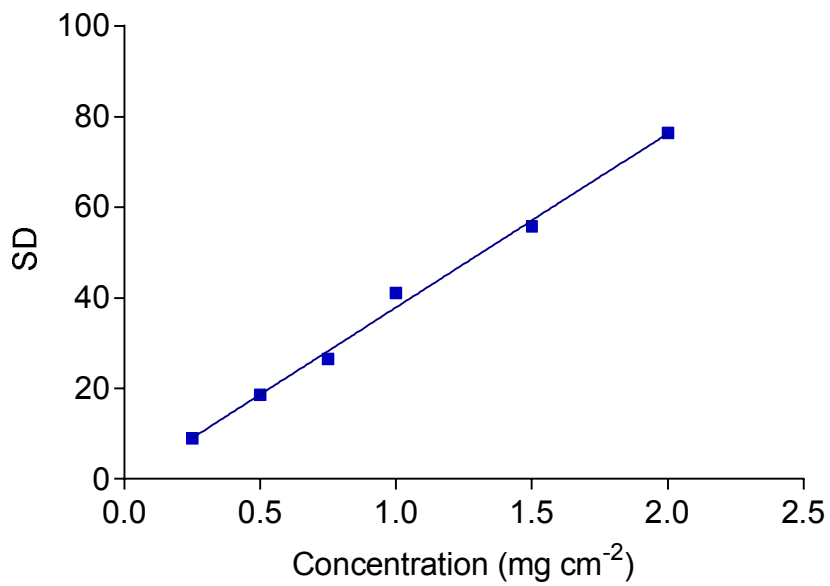
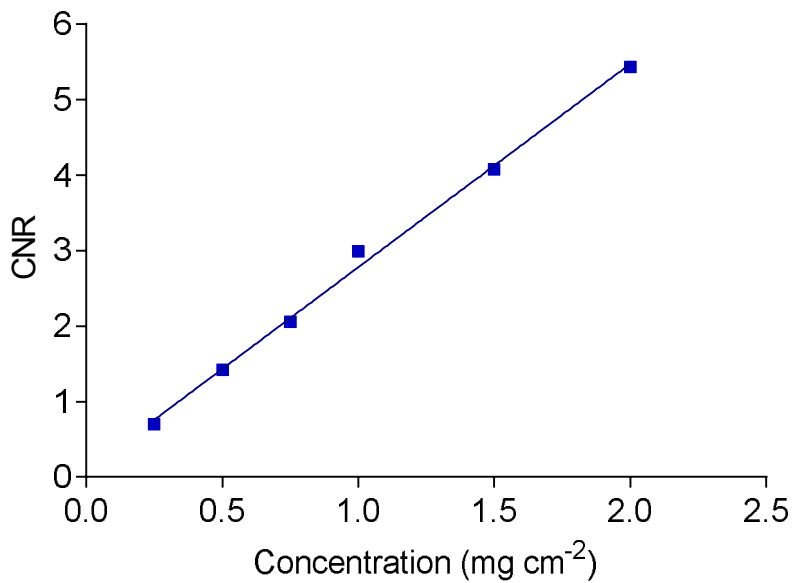


Figure 7. CNR with varying phantom thickness for different concentrations of iodine (mg cm<sup>-2</sup>)



**Figure 8. SD with varying iodine concentration for 50 mm thick phantom**



**Figure 9. CNR with varying iodine concentration for 50 mm phantom thickness**

### 3.6. Mean glandular dose

The MGDs for the tissue equivalent blocks with and without the CEM phantom acquired under “AOP STD” AEC are shown in tables 7 and 8 respectively. The value of  $s$  used in the calculation of MGD for the Mo/Cu and Rh/Cu target filter combinations was 1.0.

**Table 7. MGDs for exposures carried out using CEM phantom with additional tissue equivalent material**

Phantom thickness (mm)	Glandularity (%)	Exposure parameters (kV Target/Filter)		Calculated MGD (mGy)		
		Low energy exposure	High energy exposure	Low energy exposure	High energy exposure	Total
20	97	26 Mo/Mo, 19.1 mAs	49 Mo/Cu, 51.1 mAs	0.53	0.37	0.90
30	76	26 Mo/Mo, 41.8 mAs	49 Mo/Cu, 78.6 mAs	0.89	0.55	1.44
40	52	34 Rh/Ag, 23.9 mAs	49 Rh/Cu, 119 mAs	1.18	0.89	2.07
50	34	34 Rh/Ag, 29.5 mAs	49 Rh/Cu, 113.1 mAs	1.32	0.82	2.14
60	22	34 Rh/Ag, 37.2 mAs	49 Rh/Cu, 115 mAs	1.51	0.81	2.32
70	18	34 Rh/Ag, 47.9 mAs	49 Rh/Cu, 116.8 mAs	1.77	0.79	2.56

**Table 8. MGDs for exposures carried out using tissue equivalent material only**

Phantom thickness (mm)	Glandularity (%)	Exposure parameters (kV Target/Filter)		Calculated MGD (mGy)		
		Low energy exposure	High energy exposure	Low energy exposure	High energy exposure	Total
20	100	26 Mo/Mo, 18.6 mAs	49 Mo/Cu, 50.6 mAs	0.52	0.37	0.88
30	70	26 Mo/Mo, 39.4 mAs	49 Mo/Cu, 77 mAs	0.84	0.54	1.38
40	50	34 Rh/Ag, 23.5 mAs	49 Rh/Cu, 120 mAs	1.16	0.90	2.06
50	33	34 Rh/Ag, 28.8 mAs	49 Rh/Cu, 114.9 mAs	1.28	0.84	2.12
60	21	34 Rh/Ag, 35.7 mAs	49 Rh/Cu, 114.4 mAs	1.45	0.81	2.26
70	12	34 Rh/Ag, 45.3 mAs	49 Rh/Cu, 117.8 mAs	1.67	0.80	2.48
80	7	34 Rh/Ag, 61.3 mAs	49 Rh/Cu, 116.3 mAs	2.11	0.76	2.88
90	4	34 Rh/Ag, 84.2 mAs	49 Rh/Cu, 125.6 mAs	2.70	0.79	3.50

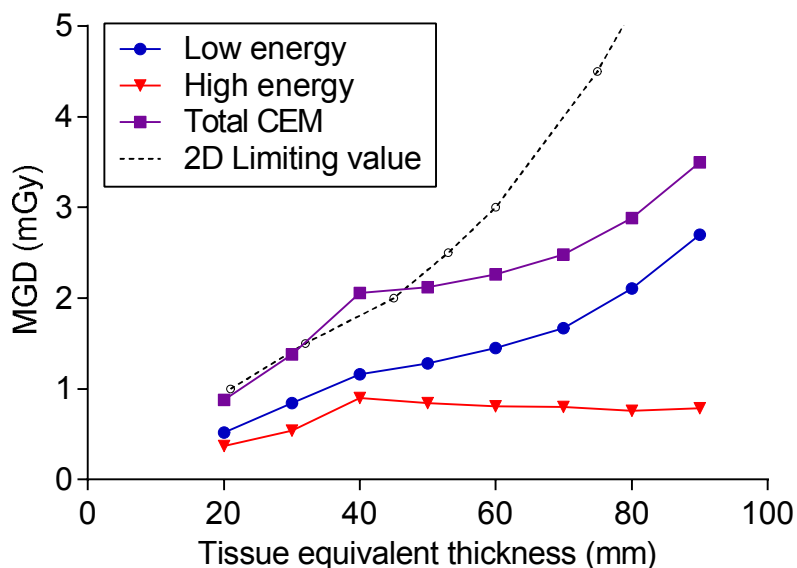


Figure 10. MGD for tissue equivalent material

The MGDs for tissue equivalent material are shown in Figure 10. CEM is a different imaging modality from standard 2D imaging and so the limiting dose values are not relevant, but it is of interest to compare them. It can be seen that the calculated total MGD is above the limiting dose value for 2D screening for the 40 mm thick blocks.

### 3.7. Accuracy of Indicated MGD

Table 9. Accuracy of indicated MGD

Phantom thickness (mm)	MGD (mGy) for low energy exposure			MGD (mGy) for high energy exposure			Difference for total MGD
	Calculated	Indicated	Difference	Calculated	Indicated	Difference	
20	0.52	0.52	0.4%	0.37	0.36	-1.5%	-0.4%
30	0.84	0.82	-2.4%	0.54	0.53	-1.6%	-2.1%
40	1.16	1.26	8.9%	0.90	0.90	-0.2%	4.9%
50	1.28	1.37	6.6%	0.84	0.84	0.5%	4.2%
60	1.45	1.53	5.3%	0.81	0.82	1.7%	4.0%
70	1.67	1.85	10.5%	0.80	0.81	1.1%	7.5%
80	2.11	2.26	6.9%	0.76	0.77	0.9%	5.3%
90	2.70	2.83	4.7%	0.79	0.81	2.0%	4.1%

Table 9 shows the difference between the calculated MGD and the MGD shown by the system for tissue equivalent material only. The maximum difference between the indicated and calculated MGDs was 10.5% for the low energy exposure, 2.0% for the high energy exposure and 7.5% for the total MGD.

### 3.8. Comparison of MGD between Low Energy CEM and Standard 2D Images

The system uses the same factors for the low energy CEM and standard 2D exposures.

### 3.9 Subtraction of BR3D Tissue-Equivalent Material

Figure 12 demonstrates the successful subtraction of the tissue-like structures in the CIRS BR3D phantom (Figure 11) to reveal the iodine samples.

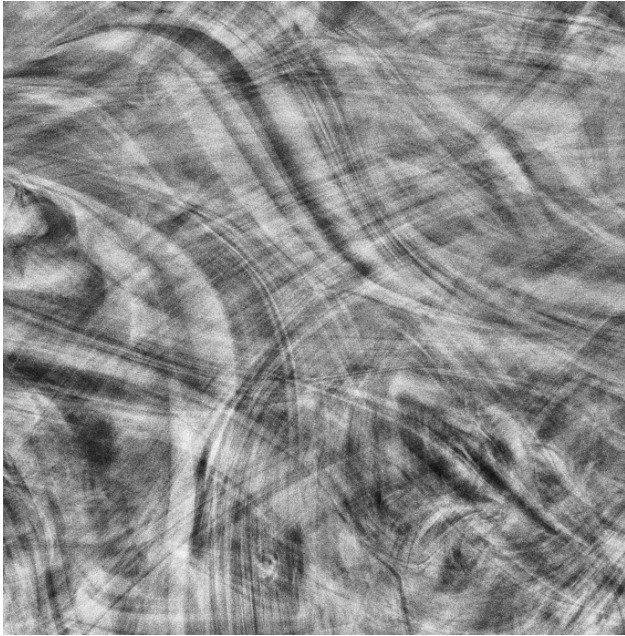


**Figure 11. Low energy image of iodine samples with BR3D material**

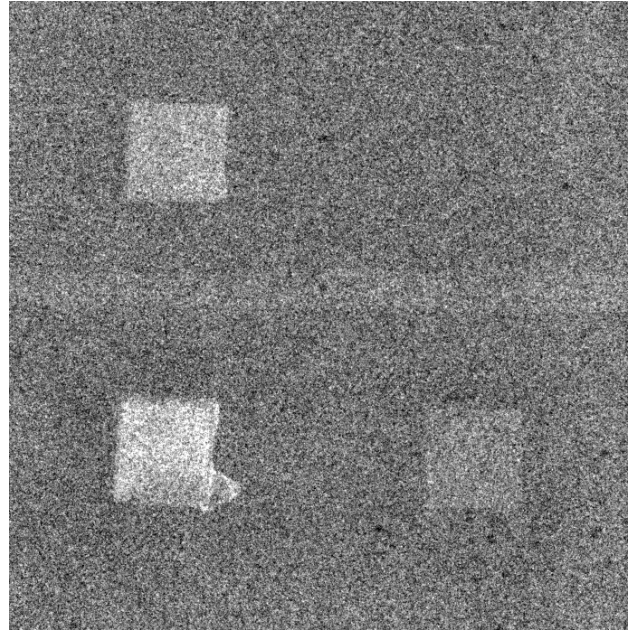


**Figure 12. Subtracted image of iodine samples with BR3D material**

## 4. Discussion

### 4.1 Detector response and uniformity

- Image pixel value and variance are linear with mAs (and hence detector dose).
- Percentage non-uniformity measured using an unprocessed high energy image of the contrast phantom was 1.2%. Only minor artefacts were seen, which are not expected to be seen on clinical images

### 4.2 Automatic exposure control

- Exposures in “AOP STD” AEC mode were repeatable in terms of mAs, SD and CNR.
- Exposure parameters (kV, target and filter) are the same for low energy CEM exposures and standard 2D exposures.

### 4.3 Mean glandular dose

- The MGD for the 50 mm thick phantom was 1.28 mGy and 0.84 mGy for the low and high energy contrast imaging exposure respectively.
- The total MGD for a CEM exposure is between 1.3 and 1.8 times the MGD of the low energy exposure alone for phantom thicknesses ranging from 20 mm to 90 mm. The total MGDs are generally below the dose limiting values for 2D screening mammography.
- The maximum deviation between the indicated and calculated MGD was 10.5% for the low energy CEM exposure and 2.0% for the high energy CEM exposure, with a maximum error of 7.5% for the total MGD.

### 4.4 Image quality

- For all iodine concentrations, the SD remains relatively constant with increasing phantom thickness when imaged in “AOP STD” AEC mode. The CNR initially increases and then decreases with increasing phantom thickness, although CNRs are within  $\pm 15\%$  of the mean across the range of phantom thicknesses for 1.0 mg cm<sup>-2</sup> iodine. The SD and CNR increase linearly with iodine concentration for any given phantom thickness.

### 4.5 Image subtraction

- The system was able to successfully subtract the tissue-like structures in the BR3D material to reveal the iodine samples imaged.

## 5. Conclusions

The system was found to be operating satisfactorily. Variations in SD and CNR with iodine concentration and phantom thickness follow similar trends to those seen in published data.<sup>1,2</sup>

## References:

1. Oduko, J., Homolka, P., Jones, V. and Whitwam, D. A Protocol for Quality Control Testing for Contrast-Enhanced Dual Energy Mammography Systems. In: Fujita H., Hara T. and Muramatsu C. eds. *IWDM 2014: Breast Imaging, 29 June – 2 July 2014*, Gifu City, Japan. Switzerland: Lecture Notes in Computer Science, Springer, Cham. 8539, pp. 407-414.
2. Oduko, J., Homolka, P., Jones, V. and Whitwam, D. Dose and Image Quality Measurements for Contrast-Enhanced Dual Energy Mammography Systems. Proceedings of SPIE, Medical Imaging 2015: Physics of Medical Imaging. Proceedings of SPIE. 2015, 9412, 94125I-1.
3. Oduko JM, Mackenzie A. Technical evaluation of GE Senographe Pristina digital mammography system in 2D mode (NHSBSP Equipment Report). London: Public Health England, 2019.
4. Leithner R, Knogler T, Homolka P. Development and production of a prototype iodine contrast phantom for CEDEM, *Physics in Medicine and Biology*, 2013, 58, N25-35.
5. Dance, D.R., Skinner, C.L., Young, K.C., Beckett, J.R. and Kotre, C.J. Additional factors for the estimation of mean glandular breast dose using the UK mammography dosimetry protocol. *Physics in Medicine and Biology*. 2000, 45, pp. 3225–3240.
6. Moore AC, Dance DR, Evans DS et al. The Commissioning and Routine Testing of Mammographic X-ray Systems. York: Institute of Physics and Engineering in Medicine, Report 89, 2005.
7. Kulama E, Burch A, Castellano I et al. *Commissioning and routine testing of full field digital mammography systems* (NHSBSP Equipment Report 0604, Version 3). Sheffield: NHS Cancer Screening Programmes, 2009.
8. Dance, D.R. and Young, K.C. Estimation of mean glandular dose for contrast enhanced mammography: factors for use with the UK, European and IAEA breast dosimetry protocols. *Physics in Medicine and Biology*. 2014, 59, pp. 2127–2137.